*Original Scientific Paper*
*CCA-1664* UDC 541
YU ISSN 0011-1643

# Bond Energies of Nitrogen and Phosphorous Hydrides and Fluorides

*J. Berkowitz, S. T. Gibson, J. P. Greene, O. M. Nešković*, and B. Ruščić†*

*Argonne National Laboratory, Argonne, IL 60439, U.S.A.*

Received September 5, 1985

Recent measurements of bond energies in the N—$H_n$ and P—$H_n$ systems by photoionization mass spectrometry are compared with modern ab initio calculations and a semi-empirical theory. Good agreement is noted, providing confirmation for the level of accuracy of the ab initio calculations, and for the essential correctness of the semi-empirical parametrization. However, the N—$F_n$ and P—$F_n$ systems, also measured, are currently beyond the capabilities of such high quality ab initio calculations, and the trends observed in the bond energies indicate that other parametrizations are necessary in the semi-empirical approach.

## I. INTRODUCTION

Modern ab initio quantum chemical calculations utilizing large basis sets and configuration interaction or Møller-Plesset perturbation theory are achieving (in certain selected cases) accuracies of ± 2 kcal/mol for bond energies (heats of formation) and ± 0.1 eV for ionization potentials.[1] Precise experimental data are lacking in some instances to test these calculations. While it is reassuring to now have a powerful mathematical apparatus available for calculating thermochemical properties of certain small molecules to acceptable chemical accuracy, it is still desirable to extract some generalizations and simplifications that may be transferable. Many years ago, Pauling[2] proposed the concept of average bond energies, and his tables have been extensively used by chemists. With the current experimental and theoretical capabilities, we are beginning to see significant variations from this average bond energy. Goddard and Harding[3] have shown that the ordering of bond energies in many simple hydrides is governed by the one center p-p′ exchange integrals. Thus, they are able to predict that $D_o$(M—H) < $D_o$(HM—H) < $D_o$($H_2$M—H) for M = N, P, As and Sb, and that $D_o$(X-H) < $D_o$(HX—H) for X = O, S, Se and Te. Motivated in part by the need for accurate experimental data to compare with the ab initio calculations and the semi-empirical generalizations, we have embarked upon a series of experiments using the photoionization mass spectrometric (PIMS) technique.

* Boris Kidrič Institute of Nuclear Sciences — Vinča, Beograd Yugoslavia
† Rugjer Bošković Institute, Zagreb, Yugoslavia.

## II. PRINCIPLE OF THE METHOD

In most instances, the heats of formation of stable molecular species such as $NH_3$, $PH_3$, $NF_3$, $PF_3$, $H_2O$, $H_2S$, etc. have been measured with high precision using calorimetric methods. Indeed, this provides the means for computing an average bond energy. However, the step-wise bond energies are more difficult to determine, because they invariably involve transient species, or free radicals, which cannot be handled by the standard calorimetric techniques. One direct approach is to excite a molecule such as $NH_3$, and detect the initial appearance energy of the neutral fragments $NH_2$ and H. This can in principle be negotiated by electron impact excitation or by electromagnetic radiation. Nowadays, the onset of fragment formation may be detected by laser-induced fluorescence, for example, but it is still a difficult technique. Alternatively, one may look for the onset of spontaneous fluorescence from a fragment, signalling the initial appearance of the excited fragment species. By subtracting the fluorescence energy, one can arrive at a bond dissociation energy. This latter experiment is simple in principle, but apparently difficult in general application. A modest extension of such an experiment is to produce an ionic fragment, i. e.

$$AB + E \rightarrow A^+ + B + e. \tag{1}$$

The energy onset of the fragment can now be detected with high sensitivity, since even a single charged particle can be measured. The excitation energy $E$ can be provided by various sources, including electron and ion impact, and charge exchange. At the present time, the most controlled and precise excitation source is photon impact. The energy can be monochromatized to high resolution, it can be tuned, and the ion yield of $A^+$ frequently increases linearly from threshold, enabling one to extract a fairly accurate threshold. The method is applicable to most molecular species. An important assumption made in the application of this method is that the threshold measured is, in fact, the true thermochemical treshold. This is often, but not invariably the case.

In order to deduce a bond energy, it is necessary to determine an adiabatic ionization potential for A, which generally is a reactive, transient species. This is usually the difficult part of the method. One must devise a scheme for generating A in sufficient abundance to make measurements of the ionization yield, and hence the adiabatic threshold, possible. In the past, controlled electron impact has been used to determine the onset of $A^+$ from A. This method is limited by the threshold behavior of electron impact ionization, which is less abrupt than photoionization, and also by the usually lower energy resolution of electron beams compared to photon beams. Photoelectron spectroscopy can achieve fairly high energy resolution in favorable cases, but without mass resolution one is often plagued by a superposition of photoelectron spectra from various species simultaneously produced, including the starting reagents used to generate the transient species. Photoionization mass spectrometry enables one to focus attention on the species of interest, and to look for the onset of the process

$$A + h\nu \rightarrow A^+ + e, \tag{2}$$

which is the adiabatic ionization potential.

Then, a simple subtraction of the onset energy of reaction (2) from that of reaction (1) yields the bond energy A—B.

## III. EXPERIMENTAL METHODS

### A. Photoionization Mass Spectrometry

The apparatus we are currently using has been described previously.[4] It consists of a broad-banded vacuum ultraviolet (VUV) light source, a 3m VUV monochromator, an ion source where the VUV radiation traverses the gaseous target, a detector for the VUV radiation, some ion optics directing the ions formed into a quadrupole mass spectrometer, and an ion detector.

We have mostly utilized laboratory discharge light sources, which provide a continuum or quasi-continuum between ~600—2000 Å. Synchrotron radiation is an obvious alternative. There are many pros and cons concerning the choice of light source, but such details are beyond the scope of the present article.

### B. Preparation of Transient Species

There are three general techniques which we have found to be useful in generating transient species — pyrolysis, electric discharge and chemical reaction. We are currently investigating a fourth, photolysis.

#### 1. Pyrolysis

The design we have used is shown in Figure 1. Concentric quartz tubes are employed. The parent molecular species must be thermochemically unstable and yield the desired transient product in the temperature range achievable with a quartz reactor, ~1000 °C. The gas enters through the innermost tube, is heated in two sections, and flows directly into the ionization region. The ionization chamber is »open«, enabling the molecular beam to pass directly through, and on into the throat of a liquid nitrogen trap and diffusion pump. The temperature of the reactor is controlled by resistively heating tungsten ribbon wound in spiral fashion around a quartz tube which slides adjustably around the innermost tube. The temperature can be monitored with a thermocouple. This procedure has been used to produce $NF_2$[5] from thermal decomposition of $N_2F_4$, $PF_2$[5] from $P_2F_4$ and $PH_2$[6] from benzylphosphine.

#### 2. Electric Discharge

The form of electric discharge which we have found most convenient is a microwave discharge. The schematic arrangement will be apparent in the following section. We attempted to prepare $NF_2$, $PF_2$, $NH_2$ and $PH_2$ by microwave discharge through $NF_3$, $PF_3$, $NH_3$ and $PH_3$, respectively, but we could not obtain a sufficient abundance of the desired species for meaningful photoionization studies. Surprisingly, we did observe $P_2$ in the $PF_3$ discharge experiments, and obtained some preliminary data. Although not relevant for the present discussion, we have had success in preparing F,[7] Cl,[8] Br[9] and SO by this technique.

#### 3. Chemical Reaction

Thus far, we have concentrated on hydrogen abstraction reactions. The Southampton group[10] has successfully employed F atoms as reagents for generating transient species in photoelectron spectroscopic measurements, and we have also used this route. Surprisingly, however, we have found more abundant yields using H atoms as reagents. A schematic diagram of the generating tube is shown in Figure 2. Metaphosphoric acid coating is used on the walls of the generating tube to prevent recombination of H atoms, which are produced in a microwave discharge through pure $H_2$. The partialy dissociated hydrogen flows rapidly by an orifice, then through the annular tube region and into a large mechanical pump. Beneath this orifice is a cup into which the other reagent flows. A grid in this region helps to minimize the background due to charged particles coming directly from the microwave discharge. Surface properties are very important to the success of this experiment. We have obtained satisfactory yields of OH, SH, $NH_2$[11] and $PH_2$ by this technique, using $NO_2$, $H_2S$, $N_2H_4$ and $PH_3$ as reagents.

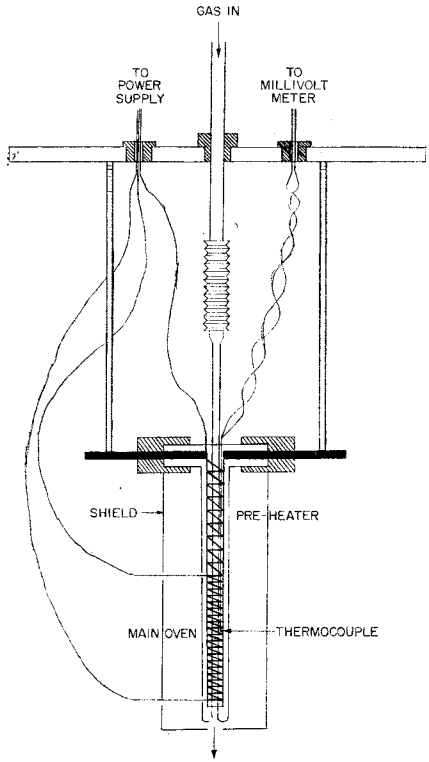


Figure 1. Schematic diagram of pyrolysis reactor used as free radical source.

## IV. EXPERIMENTAL RESULTS

### *A. The N—$H_n$ System*[11]

The photoionization mass spectrum of $NH_2$, produced by the reaction of H atoms with hydrazine, is shown in Figure 3. It is characterized by a weak onset, corresponding to the formation of $NH_2^+$ in its electronic ground state, $\tilde{X}\ ^3B_1$. A prominent Rydberg series is seen converging to the first excited state, $\tilde{A}\ ^1A_1$. This ordering of states ($^3B_1$ lower than $^1A_1$) is the same as that in the isoelectronic $CH_2$ molecule, which has received a great deal of attention recently.

In order to extract the most accurate value for the adiabatic threshold, we have attempted a fit to the threshold region assuming that its shape is determined by rotational transitions between the neutral $NH_2$ ($T \cong 300$ K) and the ion. From the best fit, we select the adiabatic *I. P.* to be (1113.0 ± ± 1.0) Å = (11.14 ± 0.01) eV. This value is 3 vibrational quanta lower than the value (11.46 eV) reported in the photoelectron spectroscopic experiment.[12] This illustrates the advantage of mass selection, since the PES experiment had to contend with a large band from $NH_3$ partially obscuring the first band of $NH_2$. However, these authors[12] were able to identify a peak in their

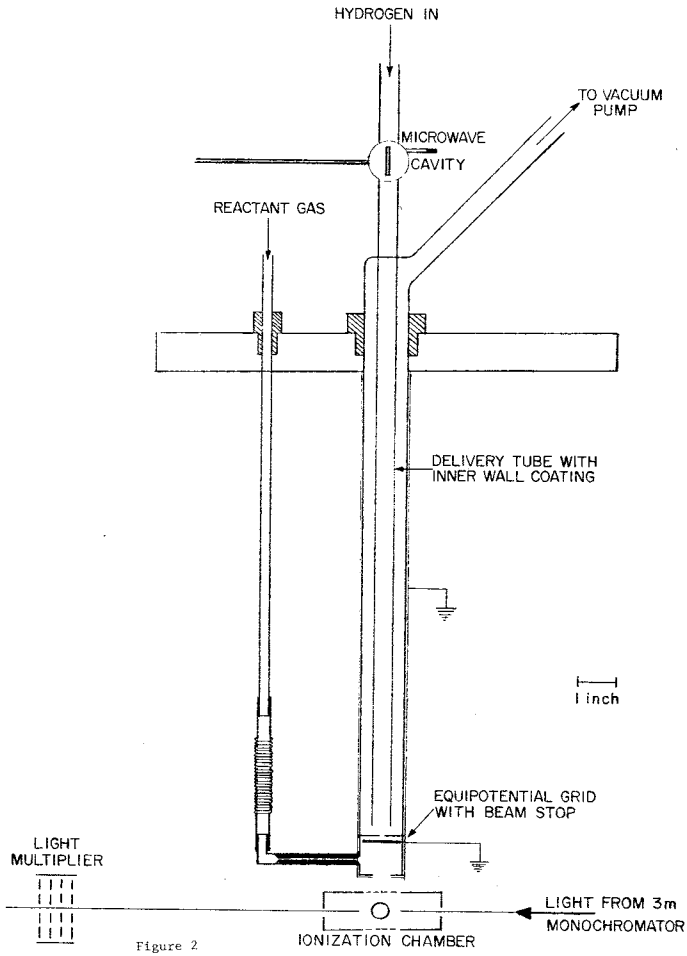


Figure 2. Schematic diagram of atom production by microwave discharge, and subsequent free radical production by chemical reaction.

spectrum corresponding to the adiabatic ionization potential of NH (also produced in their chemical reaction) at 13.49 ± 0.01 eV, which we shall utilize in the ensuing analysis.

In our PIMS experiment, we were fortunate to have enough sensitivity and freedom from various backgrounds to observe the threshold for the fragmentation process

$$NH_2 + h\nu \rightarrow NH^+ + H + e \qquad (3)$$

The ion yield curve (Figure 4) has a rather sharp threshold which (when corrected for the internal energy of $NH_2$) is 17.440 ± 0.005 eV.
Earlier, McCulloh[13] had studied the reaction

$$NH_3 + h\nu \rightarrow NH_2^+ + H + e \qquad (4)$$

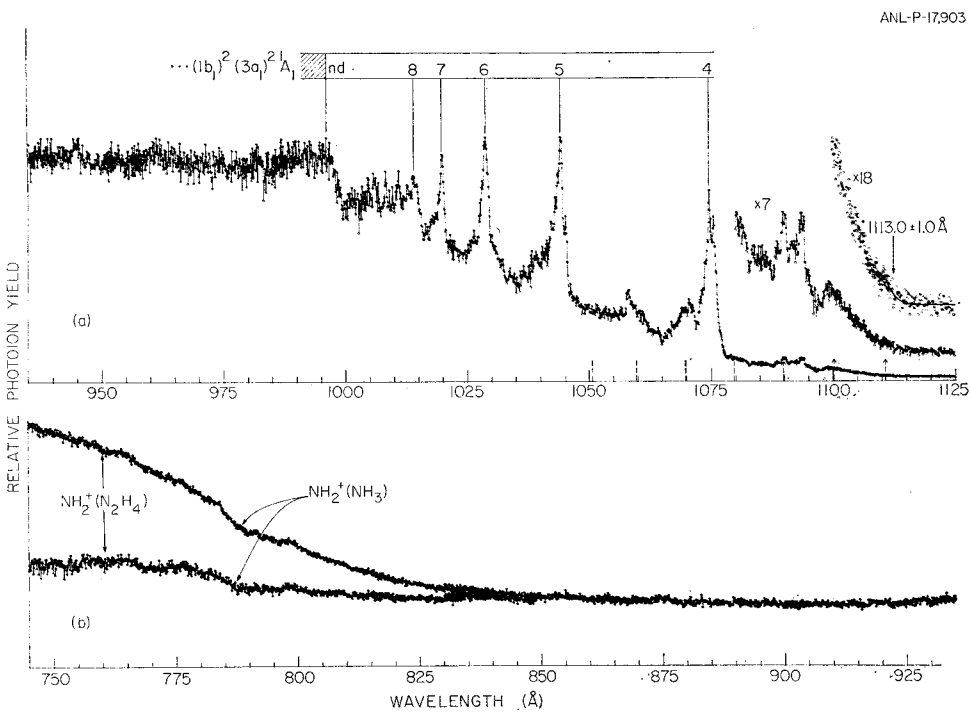


Figure 3. Photoionization yield curve of $NH_2^+$ from $NH_2$. The $NH_2$ is generated by the reaction of H atoms with $N_2H_4$. At shorter wavelengths, $NH_2^+$ is also formed from dissociative ionization of $NH_3$ and $N_2H_4$.

and obtained 15.768 ± 0.004 eV for this threshold at 0 K. When combined with the well-established values for $\Delta H_{f0}^\circ$ ($NH_3$) and $\Delta H_{f0}^\circ$ (H), we obtain $\Delta H_{f0}^\circ$ ($NH_2^+$) = 302.7 ± 0.1 kcal/mol. By subtracting the adiabatic *I. P.* ($NH_2$) = = 11.14 ± 0.01 eV found in the present work, we obtain $\Delta H_{f0}^\circ$ ($NH_2$) = = 45.8 ± 0.3 kcal/mol. This quantity, combined with the threshold for reaction (3) yields $\Delta H_{f0}^\circ$ ($NH^+$) = 396.3 ± 0.3 kcal/mol. Finally, we utilize the adiabatic *I. P.* (NH) = 13.49 ± 0.01 eV alluded to earlier to give $\Delta H_{f0}^\circ$ (NH) = = 85.2 ± 0.4 kcal/mol. These results can be utilized, together with the well-established $\Delta H_{f0}^\circ$ (N) = 112.53 ± 0.01 kcal/mol to produce the following bond energies:

$$D_0(H_2N-H) = 106.7 \pm 0.3 \text{ kcal/mol}$$

$$D_0(HN-H) = 91.0 \pm 0.5 \text{ kcal/mol}$$

$$D_0(N-H) = 79.0 \pm 0.4 \text{ kcal/mol}$$

### *B. The P—$H_n$ System*[6]

The photoion yield curve of $PH_2$, produced by the pyrolysis of benzylphosphine, is shown in Figure 5. It is significantly different from that of $NH_2$. The threshold region shows a more abrupt onset, and the sharp autoionizing Rydberg series observed in $NH_2$ is absent here. The reason for this is that the electronic ground state of $PH_2^+$ is $\tilde{X}\ {}^1A_1$ and the excited

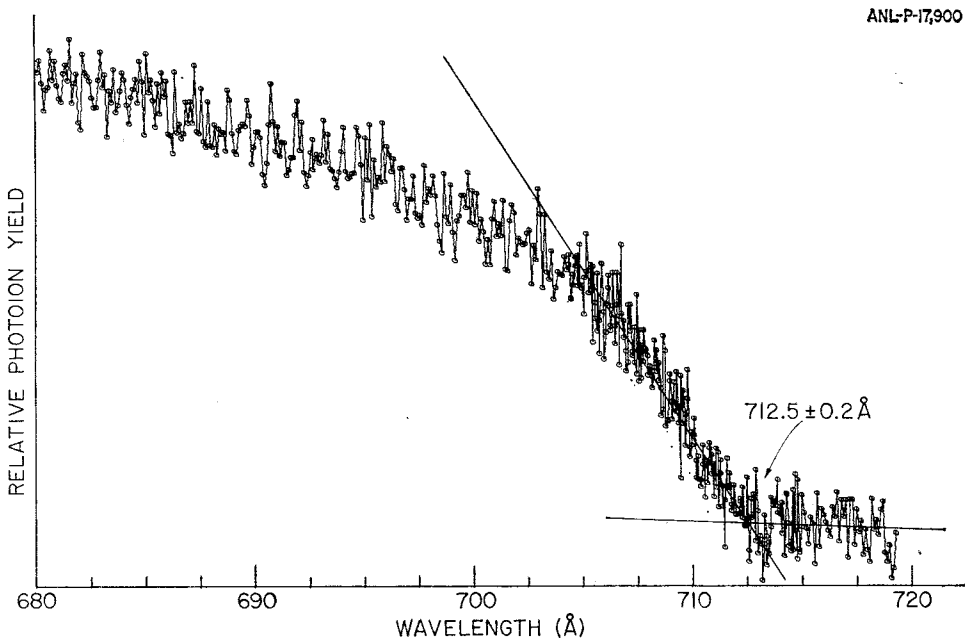


Figure 4. Photoion yield curve of $NH^+$ from $NH_2$.

state is $\tilde{A}\ ^3B_1$, just the reverse of that in $NH_2^+$ and $CH_2$. There is evidence[14] that the ordering in $PH_2^+$ is also followed in the isoelectronic $SiH_2$, and hence that the second row hydrides differ characteristically from the first row hydrides. The threshold region, again fitted by an asymmetric rotor excitation function, yields $(1262.0_5 \pm 0.3)$ Å $= (9.824 \pm 0.002)$ eV.

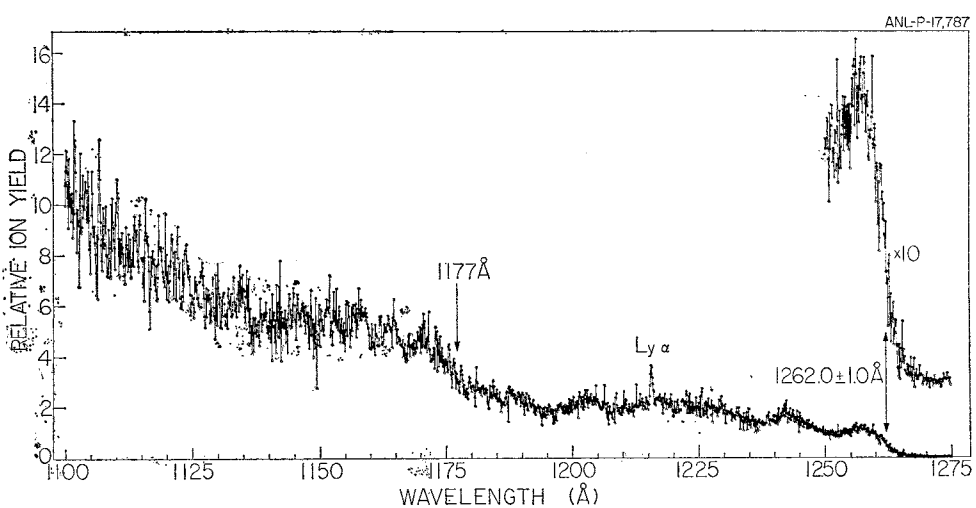


Figure 5. Photoion yield curve of $PH_2^+$ from $PH_2$. The $PH_2$ is generated by pyrolysis of benzylphosphine.

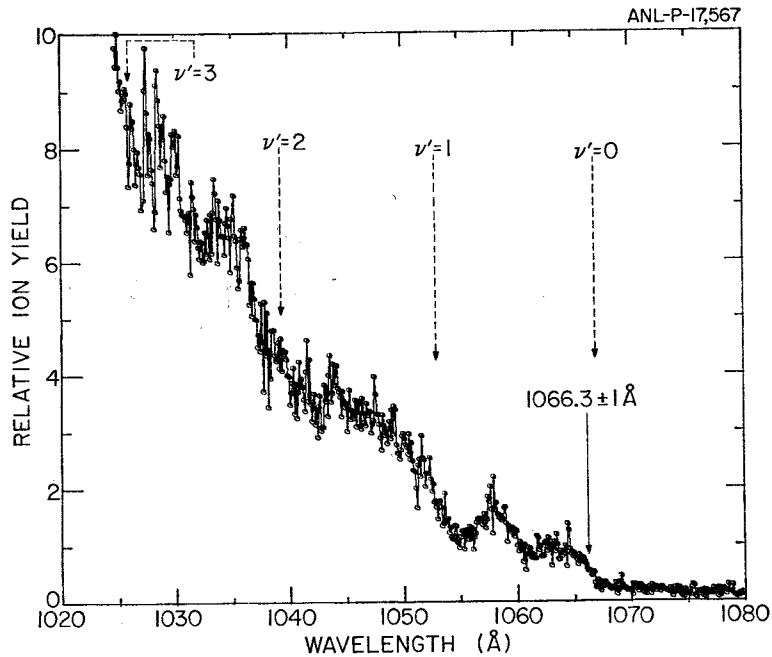


Figure 6. Photoion yield curve of $NF_2^+$ from $NF_2$. The $NF_2$ is generated by pyrolysis of $N_2F_4$. (From J. Chem. Phys. **81** (1984) 6166 with permission).

It turns out that the molecule $PH_3$ lends itself to the study of two fragmentation processes,

$$PH_3 + h\nu \rightarrow PH_2^+ + H + e \tag{5}$$

and

$$PH_3 + h\nu \rightarrow PH^+ + H_2 + e \tag{6}$$

whereas the analog to reaction (6) is very weak or absent in the case of $NH_3$. We have measured the ion yield curves corresponding to these reactions, and obtain 13.40 ± 0.02 eV for the threshold of reaction (5), and 12.492 ± ± 0.005 eV for the threshold of reaction (6), both corrected to 0 K. The additional piece of information we require is *I. P.* (PH).

In a review paper, Dyke, et al.[10] recorded the photoelectron spectra resulting from the reaction of F atoms with $PH_3$ at three mixing distances above the photon beam. They assigned these complex spectra to various superpositions of $PH_3$, $PH_2$, PH, P, $P_2$, PF, $PF_2$ and $O_2$. They did not discuss the peaks assigned to PH. Our reading of the lowest energy peak they assign to PH yields *I. P.* (PH) = 10.17 — 10.18 eV.

Now, proceeding as in Sec. IV. A., we can deduce $\Delta H_{f0}^\circ(PH_2^+) =$ $= 260.0 \pm 0.6$ kcal/mol from reaction (5), utilizing a calorimetric value[15] for $\Delta H_f^\circ(PH_3)$. Similarly, we obtain $\Delta H_{f0}^\circ(PH^+) = 291.3 \pm 0.4$ kcal/mol from reaction (6). Now making use of *I. P.* $(PH_2) = 9.824 \pm 0.002$ eV and *I. P.* (PH) = 10.17 — 10.18 eV, we obtain $\Delta H_{f0}^\circ(PH_2) = 34.0 \pm 0.6$ kcal/mol and $\Delta H_{10}^\circ(PH) = 56.6 \pm 0.5$ kcal/mol. We can combine these results, together

with $\Delta H_{f0}^{\circ}(P, g) = 75.42 \pm 0.17$ kcal/mol[16] to obtain the following bond energies:

$$D_0(H_2P-H) = 82.46 \pm 0.46 \text{ kcal/mol}$$

$$D_0(HP-H) = 74.2 \pm 0.8 \text{ kcal/mol}$$

$$D_0(P-H) = 70.5 \pm 0.5 \text{ kcal/mol}$$

The latter two values are subject to the following caveats:

(1) The calorimetric $\Delta H_f^{\circ}(PH_3)$ comes from the work of a single group,[15] and hence is not as well established as $\Delta H_f^{\circ}(NH_3)$.

(2) The threshold for reaction (5) displays some curvature, and hence may only be an upper limit. If the true threshold is lower, it will increase $D_0(HP-H)$ and correspondingly decrease $D_0(P-H)$.

Neither of these uncertainties affects the value given for $D_0(H_2P-H)$.

### C. The $N-F_n$ System[5]

The ion yield curve from photoionization of $NF_2$ (produced by pyrolysis of $N_2F_4$) is displayed in Figure 6. An analysis of the threshold region yields an adiabatic *I. P.* of $(1066.3 \pm 1.0)$ Å $= (11.63 \pm 0.001)$ eV. In this case, a photoelectron spectrum without interfering background has been recorded by Cornford, et al.[17], and they obtained *I. P.* $(NF_2) = 11.62 \pm 0.02$ eV.

With the $NF_2$ sample, it was also possible to measure the ion yield curve for the process

$$NF_2 + h\nu \rightarrow NF^+ + F + e, \tag{7}$$

which is shown in Figure 7. At 0 K, this threshold energy is $15.09 \pm 0.01$ eV. We have also re-measured the ion yield curve for the process

$$NF_3 + h\nu \rightarrow NF_2^+ + F + e \tag{8}$$

previously reported by Dibeler and Walker.[18] We obtain $14.10 \pm 0.01$ eV at 0 K for this threshold, in reasonably good agreement with that reported earlier, $14.12 \pm 0.01$ eV.

The last piece of information required for this analysis is *I. P.* (NF), which has been reported by Dyke, et al.[19] to be $12.26 \pm 0.01$ eV by photoelectron spectroscopy.

Proceeding as in Sec. IV. A, B, and with well-established auxiliary thermochemical values, we deduce $\Delta H_{f0}^{\circ}(NF_2^+) = 276.5 \pm 0.5$ kcal/mol, $\Delta H_{f0}^{\circ}(NF_2) = 8.3 \pm 0.5$ kcal/mol, $\Delta H_{f0}^{\circ}(NF^+) = 338.3 \pm 0.5$ kcal/mol and $\Delta H_{f0}^{\circ}(NF) = 55.6 \pm 0.5$ kcal/mol. These in turn can be combined to give

$$D_0(F_2N-F) = 57.0 \pm 0.2 \text{ kcal/mol}$$

$$D_0(FN-F) = 65.7 \pm 0.5 \text{ kcal/mol}$$

$$D_0(N-F) = 75.4 \pm 0.5 \text{ kcal/mol}$$

### D. The $P-F_n$ System[5]

$PF_2$ was generated by pyrolysis of $P_2F_4$. A limited sample of $P_2F_4$ was available, and the resulting ion yield curve (Figure 8) does not have the

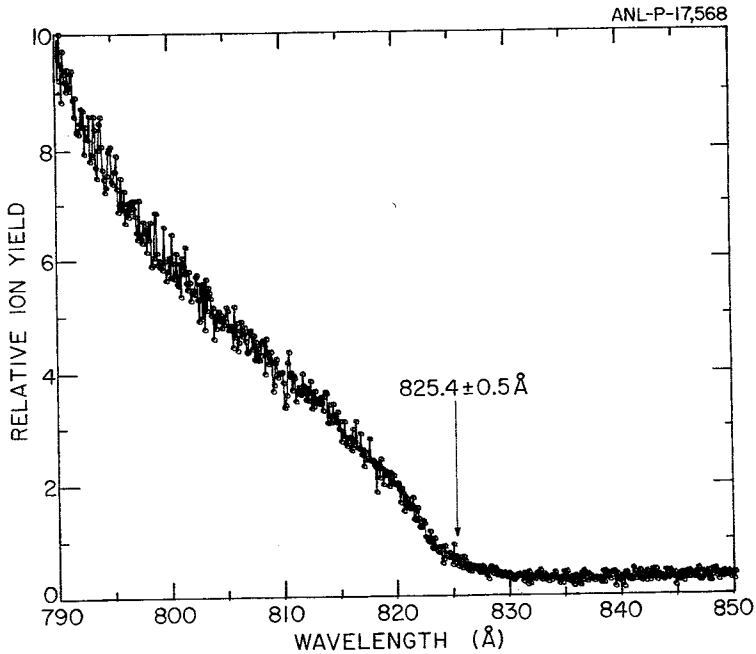


Figure 7. Photoion yield curve of $NF^+$ from $NF_2$. (From *J. Chem. Phys.* **81** (1984) 6166, with permission).

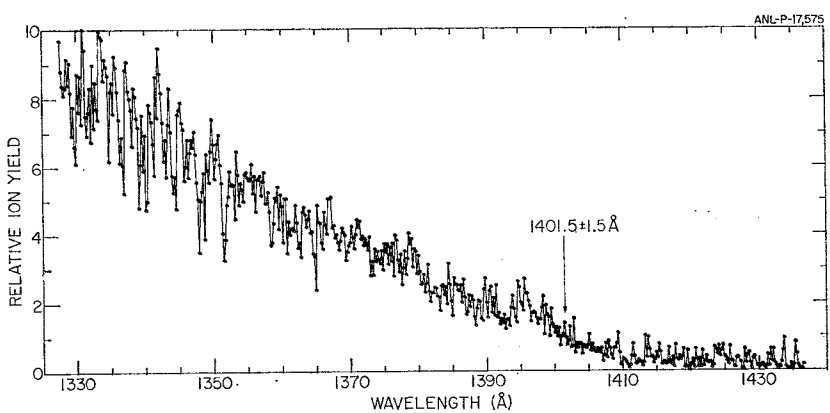


Figure 8. Photoion yield curve of $PF_2^+$ from $PF_2$. The $PF_2$ is generated by pyrolysis of $P_2F_4$. (From *J. Chem. Phys.* **81** (1984) 6166, with permission).

good signal-to-noise ratio of the earlier data presented. We extracted a value of (140.5 ± 1.5) Å = ($8.84_7$ ± 0.01) eV for the adiabatic inonization potential.

In Sec. IV. B we alluded to a complex photoelectron spectrum given in a review paper by Dyke, et al.[10] from which we extracted *I. P.* (PH). From this spectrum we can also estimate an adiabatic *I. P.* ($PF_2$) ≅ 8.82 eV.

In addition, these authors[10] provide a vertical *I. P.* (PF) = 9.74 ± 0.01 eV, and a vibrational spacing of 1030 ± 30 $cm^{-1}$, from which we can compute an adiabatic *I. P.* (PF) = 9.61 ± 0.01 eV.

The ion yield curve for the reaction

$$PF_3 + h\nu \rightarrow PF_2^+ + F + e \tag{9}$$

was measured in this sequence of experiments, and we obtained $14.55_4 \pm$ ± 0.01 eV for this threshold at O K. However, to arrive at $\Delta H_f^\circ(PF^+)$ we had to resort to a less direct measurement, because the onset for the reaction

$$PF_3 + h\nu \rightarrow PF^+ + 2F + e \tag{10}$$

is below 600 Å, which is the lower limit of our laboratory continuum light source. Such a direct experiment could be performed at a synchrotron. Instead, we used $PF_2I$ as an indirect means to our goal. The ion yield curves we examined correspond to the processes

$$PF_2I + h\nu \rightarrow PF_2^+ + I + e \tag{11}$$

and

$$PF_2I + h\nu \rightarrow PF^+ + F + I + e \tag{12}$$

The energy difference between the thresholds of reactions (12) and (11), i. e. 17.396 eV — 11.165 eV = 6.231 eV, is thermochemically equivalent to the reaction

$$PF_2^+ \rightarrow PF^+ + F. \tag{13}$$

The approach to threshold of reaction (12) is asymptotic, and hence the value 17.396 eV should be regarded as an upper limit. These observations lead to the following conclusions: $\Delta H_{f0}^\circ(PF_2^+) = 89.6 \pm 0.4$ kcal/mol from the threshold of reaction (9). When combined with *I. P.* $(PF_2) = 8.84_7$ eV (or perhaps 8.82 eV), we obtain $\Delta H_{f0}^\circ(PF_2) = -114.4$ to $-113.8$ kcal/mol. From reaction (13), $\Delta H_{f0}^\circ(PF^+) \leq 214.8$ kcal/mol; combined with *I. P.* (PF) = 9.61 ± ± 0.01 eV, this gives $\Delta H_{f0}^\circ(PF) \leq -6.8$ kcal/mol. These values can be combined to produce the following bond energies:

$$D_0(F_2P - F) = 131.7 \pm 0.5 \text{ kcal/mol}$$

$$D_0(FP - F) \leq 125.6 \pm 0.6 \text{ kcal/mol}$$

$$D_0(P - F) \geq 100.6 \text{ kcal/mol}$$

## *V. Comparison with Calculations*

In Table I, we summarize the calculated and experimental bond energies for the $N - H_n$ and $P - H_n$ compounds. The agreement between the ab initio calculations[1] and the experimental values is within the stated ±2 kcal/mol in every instance but one ($D_0(P - H)$), where the difference is 2.9 ± 0.5 kcal/mol. The agreement between experiment and the semi-empirical calculations[3] is even better for the $P - H_n$ compounds, but is distinctly poorer for the $N - H_n$ compounds, where the maximum deviation is 5.3 ± 0.03 kcal/mol. A somewhat larger value for the p-p' exchange integral would help to resolve this discrepancy.

TABLE I

*Bond Energies of N—$H_n$ and P—$H_n$ Compounds (kcal/mol)*

| | ab initio[1] | semi-empirical[2] | expt.[3] |
|---|---|---|---|
| $D_0$ ($H_2N$—H) | 107.2 | 101.39 | 106.7 ± 0.3 |
| $D_0$ (HN—H) | 92.0 | 92.23 | 91.0 ± 0.5 |
| $D_0$ (N—H) | 77.3 | 83.07 | 79.0 ± 0.4 |
| $D_0$ ($H_2P$—H) | 81.4 | 81.11 | 82.5 ± 0.5 |
| $D_0$ (HP—H) | 75.4 | 75.69 | 74.2 ± 0.8 |
| $D_0$ (P—H) | 67.6 | 70.27 | 70.5 ± 0.5 |

[1] Ref. 1
[2] Ref. 3
[3] Present work

The overall picture is reassuring. The ab initio calculations, taken to fourth order in Møller-Plesset perturbation theory, have been tested and shown to be accurate to ± 2 kcal/mol for virtually all of the bond energies measured here. Other examples are given in the recent paper by Pople, et al.[1] While we haven't focussed on the issue of ionization potentials, the measurements reported here agree with the ab initio calculations[20] to ± 0.1 eV. These calculations clearly involve »second-row« atoms as well as »first-row« atoms. Until recently, neither experimental nor ab initio values were secure for molecules containing second row atoms. However, the ab initio calculations at this level of accuracy are still limited to one »heavy« atom.

These results also provide support for the physico-chemical model used by Goddard and Harding.[3] The bond energy increases with each successive hydrogen added, with approximately the increment they predict.

However, the experimental results on the $N-F_n$ and $P-F_n$ systems show that we cannot generalize from the hydrides to other systems. The average bond energy in the $N-F_n$ system is considerably smaller than in the $N-H_n$ system, whereas the reverse is true in the corresponding phosphorous compounds. The trend in successive bond energies is the same in the $P-F_n$ compounds as was so neatly generalized in the $N-H_n$ and $P-H_n$ compounds, but the reverse is true for the $N-F_n$ compounds. Clearly, other effects are overwhelming the simple model appropriate to the hydrides. Furthermore, it is our understanding that ab initio calculations of the accuracy reported for the »single heavy atom« compounds may be extendable with present technology to »two heavy atoms«, but become increasingly prohibitive for three and four heavy atoms.

For the time being, we must resort to chemical intuition to explain the disparate behavior of the $N-F_n$ and $P-F_n$ bond energies. From Pauling's electronegativity scale[2], $\chi$ (F) = 4.0, $\chi$ (N) = 3.0 and $\chi$ (P) = 2.1. Using Pauling's

criterion, N — F bonds have 22% ionic character and P — F bonds ~60% ionic character. We believe that this property provides a rationalization for the stepwise increase in P — F bonds. In the limit of purely ionic bonding, an electron is donated to the more electronegative partner. The cost in energy for this process (*I. P.* of donor minus electron affinity of acceptor) is more than recovered by the ensuing Coulombic attraction. If we consider the stepwise addition of F to P, the electron affinity of F is common to all steps. The variation occurs in the *I. P.* of the donor. These values are 10.49 eV (P), 9.61 eV (PF) and 8.82 — 8.85 eV ($PF_2$). Hence, as the cost of removing an electron decreases, the consequent bond energy increases.

The N — $F_n$ system is much ionic, and other factors must be influencing the reverse trend. Goddard and Harding,[3] in analyzing the related C — H and C — F bond energy patterns, focus attention on »the interaction of the doubly occupied valence orbitals of the halogen with adjacent centers.« These repulsions, lone pair or otherwise, are stronger for first row compounds like N — $F_n$ than for heavier ones like P — $F_n$ because the internuclear distances are shorter. The repulsion energy will increase with each added F atom, also in qualitative agreement with experiment. It would be pleasing if this repulsion energy could be parametrized, as in the case of the exchange energy.

If a few rules could be developed regarding the effect of ionicity and repulsion which are as simple as the exchange integral parameter, it may be possible to modify and improve Pauling's average bond energies and the additivity of bond energies without getting so cumbersome that it loses its appeal.

*Note:* When not otherwise stated, the auxiliary thermochemical data utilized in this article are from ref. 16 or from JANAF Thermochemical Tables (Dow Chemical, Midland, Mich. 1977); *J. Phys. Chem. Ref. Data* **11** (1982) 695—940.

This research was supported by the U.S. Department of Energy (Office of Basic Energy Sciences) under contract W-31-109-Eng-38 and by the U. S.—Yugoslav Joint Board for Sciencentific and Technological Cooperation through U. S. Department of Energy grant JFP 561.

REFERENCES

1. J. A. Pople, B. T. Luke, M. J. Frisch, and J. S. Binkley, *J. Phys. Chem* **89** (1985) 2198.
2. L. Pauling, *The Nature of the Chemical Bond,* 3rd ed. (Cornell University press, Ithaca, 1960).
3. W. A. Goddard III and L. B. Harding, *Ann. Rev. Phys. Chem.* **29** (1978) 363.
4. See, for example, J. Berkowitz, C. H. Batson and G. L. Goodman, *Phys. Rev. A* **24** (1981) 149, and ref. 8.
5. J. Berkowitz, J. P. Greene, J. Foropoulos, Jr. and O. M. Nešković, *J. Chem. Phys.* **81** (1984) 6166.
6. J. Berkowitz, L. A. Curtiss, S. T. Gibson, J. P. Greene, G. L. Hillhouse, and J. A. Pople, *J. Chem. Phys.* **84** (1986) 375.
7. B. Ruščić, J. P. Greene, and J. Berkowitz, *J. Phys. B* **17** (1984) 79.
8. B. Ruščić and J. Berkowitz, *Phys. Rev. Lett.* **50** (1983) 675.
9. B. Ruščić, J. P. Greene, and J. Berkowitz, *J. Phys. B* **17** (1984) 1503.
10. J. M. Dyke, N. Jonathan, and M. Morris, *Intl. Revs. in Phys. Chem.* **2** (1982) 3.
11. S. T. Gibson, J. P. Greene, and J. Berkowitz, *J. Chem. Phys.* **83** (1986) 4319.
12. S. J. Dunlavey, J. M. Dyke, N. Jonathan, and M. Morris, *Mol. Phys.* **39** (1980) 1121.

13. K. E. McCulloh, *Int. J. Mass Spec. Ion Phys.* **21** (1976) 333.
14. A. Kasdan, E. Herbst, and W. C. Lineberger, *J. Chem. Phys.* **62** (1975) 541.
15. S. R. Gunn and L. G. Green, *J. Phys. Chem.* **65** (1961) 779.
16. V. P. Glushko, L. V. Gurvich, G. A. Bergman, I. V. Veits, V. A. Medvedev, G. A. Khachkunuzov, and V. S. Yungman, *Termodinamicheski Svoistva Individualnikh Veschestv* (Nauka, Moscov, 1978), Vol. **I**, Books 1 and 2.
17. A. B. Cornford, D. C. Frost, F. G. Henning, and C. A. McDowell, *J. Chem. Phys.* **54** (1971) 1872.
18. V. H. Dibeler and J. A. Walker, *Inorg. Chem.* **8** (1969) 1728.
19. J. M. Dyke, N. Jonathan, A. E. Lewis, and A. Morris, *J. Chem. Soc. Faraday Trans 2* **78** (1982) 1445.
20. J. A. Pople, private communication; to be published.

## SAŽETAK

### Energije veza hidrida i fluorida dušika i fosfora

*J. Berkowitz, S. T. Gibson, J. P. Greene, O. M. Nešković i B. Ruščić*

Energije veza u sustavima N—$H_n$ i P—$H_n$, izmjerene fotoionizacijskom spektrometrijom masa, uspoređene su s najnovijim ab initio rezultatima i s jednom poluempirijskom teorijom. Zamjećuje se dobro slaganje, koje potvrđuje visoku razinu točnosti ab initio računa, kao i ispravnost parametrizacije poluempirijskog pristupa. Međutim, sustavi N—$F_n$ i P—$F_n$, koji su također izmjereni, trenutno nadilaze mogućnosti visokokvalitetnih ab initio računa, a izmjereni trendovi u energijama veza ukazuju da je u slučaju poluempirijskog pristupa potrebna drugačija parametrizacija.